SOME REMARKS ON FRAGILITY CURVES DERIVED USING ALTERNATIVE PROBABILISTIC DEMAND MODELS

D. Skoulidou[1,2] & X. Romão[2]

[1] Resilience Guard, Steinhausen, Switzerland, des.skoulidou@resilienceguard.ch

[2] Faculty of Engineering University of Porto, Porto, Portugal

Abstract: *This study explores potential differences in analytical fragility curves obtained when considering two alternative probabilistic demand models: one obtained using Multiple Stripe Analysis (MSA) and one obtained using Incremental Dynamic Analysis (IDA). When MSA is used, different groups of ground motions compatible with different Conditional Spectra are selected for the various stripes of the analysis, where each stripe corresponds to a different seismic intensity level. Fragility curves are next developed using the EDP-based approach, according to which the probabilities of exceeding a performance level for the different seismic intensity levels are used to fit the fragility curve. In case IDA is used, a group of EC8 spectrum-compatible ground motions is selected for the design earthquake level and then scaled to cover seismic intensities that lead to a range of structural response up to collapse. Although the IM-based approach is normally used to develop fragility curves with IDA results, the EDP-based approach is also applied in this case to remove the error associated to the different fitting technique. As such, IDA curves are post-processed to create stripes of demand data for the same seismic intensity levels as those used for the MSA, which are then used to develop the fragility curves by the EDP-based approach. Three RC frame buildings are analysed using the two alternative probabilistic demand models and fragility curves are developed for various performance levels representing different states of structural damage. Differences found in the fragility curves derived by the 2 approaches reflect the different selection and scaling assumptions made for the ground motions used to obtain each demand model and allow identifying conditions where the two demand models lead to comparable fragility curves.*

1. Introduction

Fragility curves are a fundamental component for developing risk and loss assessments of structures. Depending on the data used for their development, fragility curves can be categorised as empirical, experimental, or analytical, with the latter being the most commonly used due to lack of empirical and/or experimental data. Developing analytical fragility curves requires analysing a structural model for multiple seismic intensity levels to derive the response-intensity relationship (also known as the Engineering Demand Parameter EDP – Intensity Measure IM relationship) and subsequently post-processing the results to define the evolution of the probability of reaching a certain performance level of interest for increasing levels of seismic intensity.

There are currently three widely used Probabilistic Demand Models (PDMs) to derive the EDP-IM relationship of structures using non-linear dynamic analysis: the Incremental Dynamic Analysis IDA (Vamvatsikos and Cornell, 2002), the Multiple Stripe Analysis MSA (e.g., Jalayer and Cornell, 2009) and the cloud analysis

(Jalayer at al., 2015), while some variants thereof can also be found, as for example, back-to-back IDA (Baltzopoulos et al., 2018) and Adaptive IDA (AIDA) (Lin and Baker (2013)). Combinations of alternative PDMs have also been proposed by Chatzidaki and Vamvatsikos (2021) with a view to increase reliability. All previously mentioned PDMs require the numerical simulation of the structure under investigation to represent its structural behaviour from linear elastic up to collapse, and this structural behaviour simulation needs to use one or more groups of Ground Motions (GMs) for various intensity levels. The main differences between the alternative PDMs, which has been proven to affect the EDP-IM output, lie in the procedure for selecting group/s of GMs and for scaling them to cover the required intensity levels. In the following, only IDA and MSA will be further discussed since cloud analysis is not studied in the present research. Detailed descriptions of the three alternative models and relevant discussions can be found in existing literature (e.g., Mackie and Stojadinovic (2005), Baltzopoulos et al (2018)).

IDA requires the selection of one group of GMs that is subsequently scaled to cover the entire range of the required intensity levels, while in MSA it is common practice to select different groups of GMs for different intensity levels. While IDA provides the desired continuity in the EDP-IM relationship for each GM, MSA allows the selection of groups of GMs that are compatible with the seismic hazard of the site for each intensity level leading to physically consistent results. A second consequence of this latter approach is the control and limitation of the scaling factor (SF) used for each individual GM in MSA (the previously mentioned SF only refers to the SF that may be required during spectral matching in the selection process). In contrast to that, the use of only one group of GMs, that is the case of IDA, may lead to excessive scaling of the entire group (in addition to the SF that may be required during spectral matching in the selection process) with possible implications as presented in relevant research and briefly discussed hereafter.

Scaling a group of GM with SF as large as 10 or more has been associated with overestimation of the structural response (Luco and Bazzurro, 2007) and, as an extent, with higher than expected collapse probabilities (Davalos and Miranda, 2019). This overestimation has been attributed to the fact that the frequency content and duration of a given GM are not representative for intensities much different than the one that they have been recorder for. It is worth mentioning that in the aforementioned studies, Luco and Bazzurro (2007) selected GMs using only magnitude (M) and distance (R) criteria, while Davalos and Miranda (2019) performed the GM selection using the spectral acceleration at the first period of vibration ($Sa(T_1)$). The authors of the latter study highlighted that $Sa(T_1)$ was not a sufficient IM and that the spectral shape of the GMs should be additionally considered to control the observed bias. Contradictory results have been presented by Zacharenaki et al. (2014) who showed that the bias introduced by IDA was small and acceptable for the buildings analysed in their study. In this case, M and local soil conditions (V_{S30}) were considered for the GM selection, without spectral matching considerations, and SFs up to 18.2 were employed.

Moving beyond EDPs, comparisons of fragility curves developed based on IDA and MSA can also be found in existing literature. Pang and Wang (2021) compared fragility curves constructed from IDA and MSA results and stated that the MSA results were more accurate while the bias observed for the IDA curves was attributed to the excessive scaling of the GMs involved in IDA. For the GM selection, the authors considered only seismological parameters, such as M, R, V_{S30}, and SF restrictions, while no consideration was given to the GMs spectral shape. In a relevant study applied to arch dams, Jin et al. (2023) observed that IDA overestimated the fragility curves when excessive SFs were used compared to MSA. For the IDA, GM selection was based on M, R, V_{S30}, while for the MSA GM selection was performed based on $Sa(T_1)$ without spectral shape considerations. The proposed AIDA approach (Lin and Baker, 2013) aimed at obtaining EDPs that are hazard consistent, as in MSA, using an approach as efficient as IDA, as the authors noticed that especially for higher IM levels IDA overestimated the structural response and the probability of collapse. Korhangi et al (2017) focused on the construction of multi-site fragility curves using a more efficient and sufficient IM. The comparison of IDA and MSA results showed that the use of GMs without spectral and hazard consistency could lead to bias. In the referred study, the bias was towards overestimation for the IDA results, yet it was highlighted that the overestimation could not be generalised.

Based on the above, the SF, the sufficiency of the IM and the spectral shape control seem to be the key aspects for the discrepancies that appear between the fragility curves developed based on results from different PDMs. To provide additional insights on the matter, the present study provides further results and discusses differences found at the fragility curve level when fragility curves are constructed considering the two alternative PDM, i.e., IDA and MSA. By adopting the same fragility curve fitting technique for both PDM, the referred differences will only reflect the selection and scaling assumptions made for the GMs used to obtain each demand model. Three RC buildings are simulated and analysed according to the two alternative approaches. The response results are subsequently post-processed and fragility curves are created for several limit states. The comparison of the results identifies the conditions where the two demand models lead to comparable fragility curves as well as possible limitations of each model.

2. Case study description

2.1. Analyzed buildings and numerical modelling

Three RC buildings with infilled frame structural systems, designed for gravity loads, are analysed herein. The buildings are located in Lisbon, Portugal and comprise 3-, 4- and 5-storey buildings, regular both in plan and in elevation. Figure 1 shows the plan view of a typical storey of the buildings and the design details. The structural configuration, material characteristics, loading assumptions and the numerical simulation of the buildings have been previously presented in (Skoulidou and Romão, 2019) and are omitted here due to length restrictions.

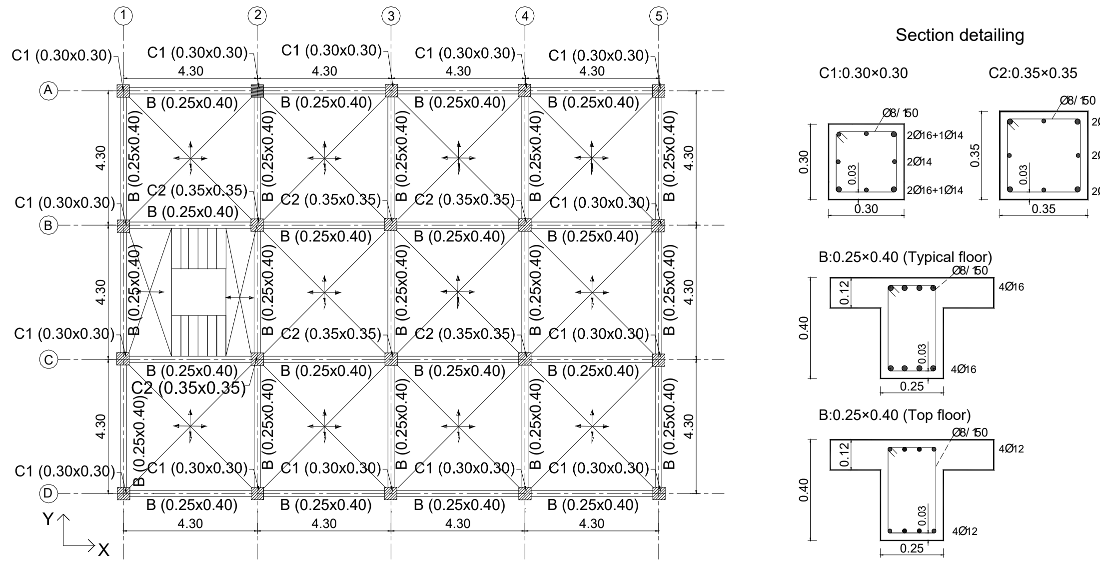

Figure 1. Plan view of a typical storey of the 3-storey, 4- storey and 5- storey buildings and the design details (all dimensions are in m).

The structural periods of the buildings along X and Y structural directions, with and without the masonry infills, as well as the average period T^* are presented in Table 1.

Table 1. First and second mode periods of vibration of the buildings.

Period (s)\Building	**3-storey**	**4-storey**	**5-storey**
T_1,T_2 (infilled frame)	0.31,0.25	0.41,0.31	0.52,0.39
T_1,T_2 (bare frame)	0.73,0.72	0.96,0.93	1.18,1.15
T^*	0.50	0.66	0.82

2.2. Ground motion selection

The ground motion selection procedures are presented in this section for the two PDMs. In both cases the geometric mean was used as the representative component for each bi-directional GM.

For the MSA, the probabilistic seismic hazard analysis of the site (Lisbon) was initially performed using the SelEQ software (Macedo and Castro, 2017) and the annual seismic hazard curve was subsequently determined for the period T^* of each building. Disaggregation of the hazard was then performed for four probabilities of exceedance, i.e., 50%, 10%, 5% and 2% in 50 years, at *T** and the results were used to build four conditional spectra (CS). After a preliminary ground motion record selection based on seismological and strong motion parameters, the final selection of a group of 40 bi-directional records was performed by ensuring compatibility between the target spectrum, i.e., the CS, and the group of records. Compatibility was achieved by minimizing the difference between statistics (i.e., the mean and standard deviation of the logarithms of the spectral accelerations) of the target spectrum and the same statistics of the group in a period range of 0.2 *T**-1.5*T** (see Macedo and Castro (2017) for more details). An additional criterion was included in the process which involves minimizing also the skewness of the logarithms of the spectral accelerations to a value close to zero for the same period range. Furthermore, the SFs used for each individual GM were restricted to the 0.25-4.00 range. Ultimately, four groups of 40 GMs, each corresponding to a different probability of exceedance (i.e., a different CS), were selected for each building.

For the IDA, one group of 40 bidirectional GM records was selected according to the EC8 provisions using the Type 2 elastic response spectrum with a 5% viscous damping. The parameters of the EC8 response spectrum used for the GM selection procedure are provided in Table 2, where a_g is the design ground acceleration for soil type A and zone 2.3 in Portugal, S is the soil factor for soil type B, and Tb, Tc and Td are the corner periods. Criteria related to seismological and strong motion parameters, such as M, R and V_{S30} were taken into account when performing the preliminary GM selection. Subsequently, the GM selection was performed by ensuring compatibility between the group mean and individual response spectra and the target response spectrum in a period range of 0.2 *T**-1.5*T**. The spectral mismatch between the mean of the group and the target response spectrum was limited to the interval of ±10%, while the spectral mismatch between the individual spectrum of each record and the target spectrum was limited to ±50%. The SFs used for each individual GM were restricted to 0.25-4.00 range.

Table 2. EC8 Type 2 response spectrum parameters.

RS	a_g (m/s^2)	S	T_b (s)	T_c (s)	T_d (s)
Type 2	1.7	1.27	0.1	0.25	2

The mean spectrum (and dispersion) of the 40 GMs matched to the CS for each probability of exceedance and the mean spectrum (and dispersion) of the 40 GMs matched to the EC8 spectrum are shown in Figure 2, Figure 3 and Figure 4 for the 3-storey, the 4-storey and the 5-storey buildings, respectively. The target CS and the EC8 spectrum are also presented in the same figures for comparison. Note that the GMs selected to match the EC8 spectrum are the same for all buildings and for all intensities. The mean spectrum of the EC8-compatible GM group, which is originally matched to the EC8 spectrum with 10% probability of exceedance in 50 years, is multiplied by appropriate SFs to reach the intensity of the other three probabilities of exceedance at Sa(*T**) for each building. In the comparison of response spectra presented in the following, focus should be given to period ranges that are expected to govern the behaviour of the structures for different damage states. Therefore, for low damages states, spectral comparisons should focus on the period range below, but close to, *T** which involve spectral values with higher probabilities of exceedance. On the contrary, for high damages states, spectral comparisons should focus on the period range above, but close to, *T** which involve spectral values with lower probabilities of exceedance.

Starting from the comparison of the target spectra, the target CS and the EC8 spectrum are seen to present some differences that vary with the probability of exceedance and with the building (i.e. *T**). Generally, the differences appear to be more pronounced for the higher probabilities of exceedance, while they reduce for the lower probabilities of exceedance for all buildings. Focusing on the lower period range (i.e., below, but close to, *T**), the CS is always associated with higher spectral accelerations for the 30% and 10% probability of exceedance in 50 years, whereas this effect reduces for the lower probabilities of exceedance. For the 2% probability of exceedance in 50 years the two spectra coincide in this period range for all three buildings. The opposite trend is observed for the higher period range (i.e., above, but close to, *T**). While for higher probabilities of exceedance the CS is associated with smaller spectral accelerations when compared to the EC8 spectrum, for the lower probabilities of exceedance this mismatch decreases and, in some cases, the trend is inverted. An illustrative example of this last observation can be seen in Figure 2d with the spectra for the 3-storey building, in which the red continuous line, i.e., the CS, is above the black continuous line, i.e., the scaled EC8 spectrum, for the referred period range.

With respect to the comparison of the mean of each group with the respective target spectra, very good matching trends are observed for the period range of interest. The EC8 compatible group follows very closely the target EC8 spectrum for the whole period range, while some deviations start appearing for periods larger than1.5 s that are beyond the period range of interest for all buildings. The CS compatible groups, on the other hand, match very well the target CS for all periods above ~0.1-0.2s. Since the lowest period of interest is 0.1s, i.e., 0.2*T** for the 3-storey building, matching is also considered adequate. As a result, it can be seen that the average spectra follow trends similar to those of the target spectra, showcasing the validity of the selection process and indicating that the differences between the mean spectra of the groups stem from the different target spectra they were matched to.

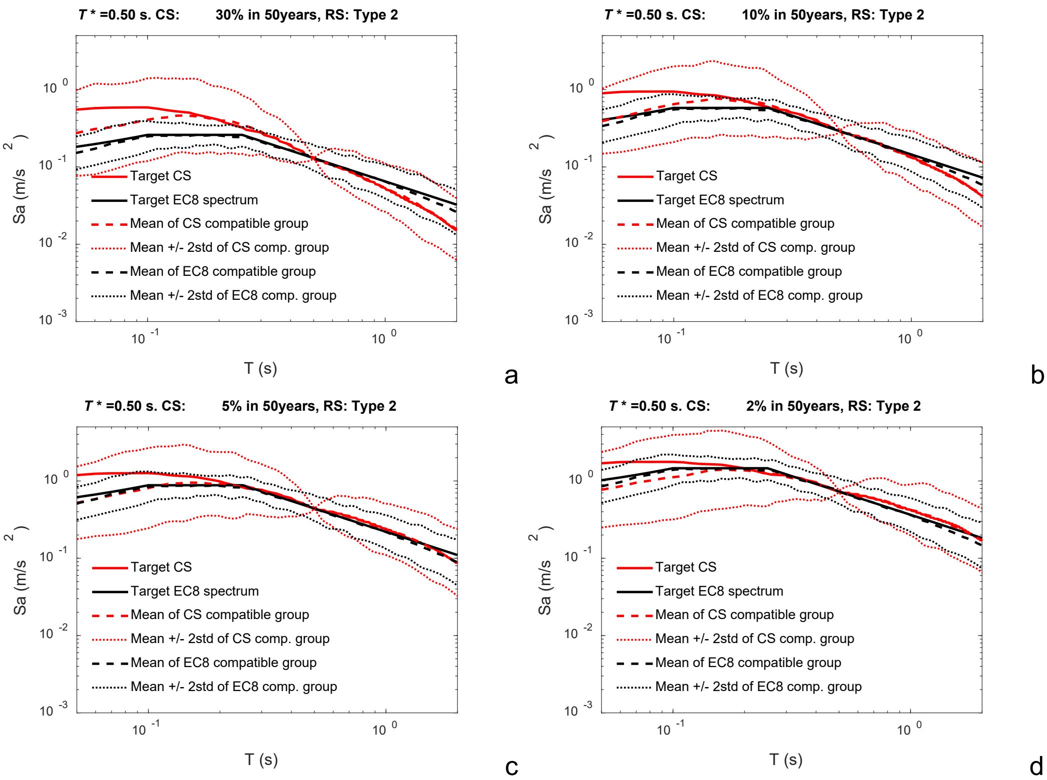

Figure 2. Comparison of response spectra (average and dispersion) of the group of GMs selected for the 3-storey building according to the CS (a. 30% in 50 years, b. 10% in 50 years, c. 5% in 50 years and d. 2% in 50 years) and the EC8 response spectrum. The target CS and EC8 spectrum are plotted for reference.

In contrast to the mean spectrum, the dispersion of the groups presents significant differences. With the exception of the narrow range very close to *T** where the CS compatible group has very low dispersion, as expected since all GMs have been selected and scaled to pass through Sa(*T**), the EC8 spectra compatible group has either comparable or much lower dispersion for all other periods, when compared to that of the CS compatible groups. Extreme cases are observed for the 30% probability of exceedance of all buildings (see Figure 2a, Figure 3a, Figure 4a), where both the mean spectrum and the dispersion have much higher Sa values for periods smaller than *T**. Unlike the previous observations, very good matching is observed, both for the mean spectra and the dispersion, for the 2% probability of exceedance CS compatible group and the EC8 spectrum compatible group of the 5-storey building (see Figure 4d). It is noted that the different dispersion between the GM groups selected according to the different approaches is due to the different assumptions considered during the GM selection process.

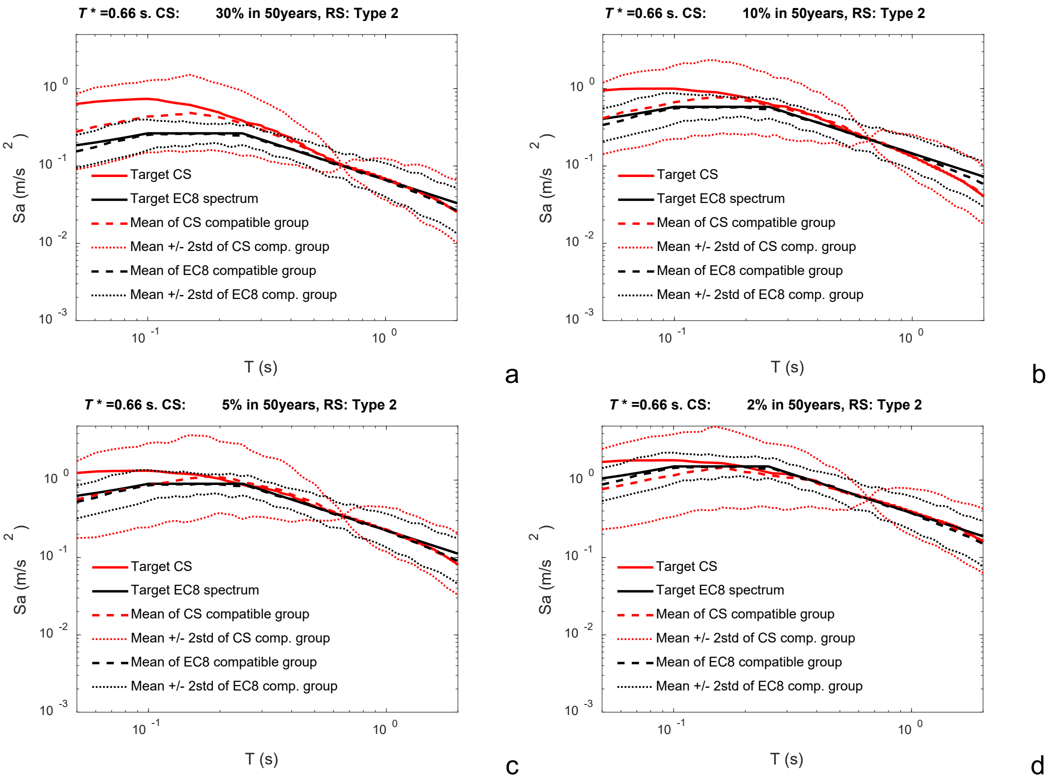

Figure 3. Comparison of response spectra (average and dispersion) of the group of GMs selected for the 4-storey building according to the CS (a. 30% in 50 years, b. 10% in 50 years, c. 5% in 50 years and d. 2% in 50 years) and the EC8 response spectrum. The target CS and EC8 spectrum are plotted for reference.

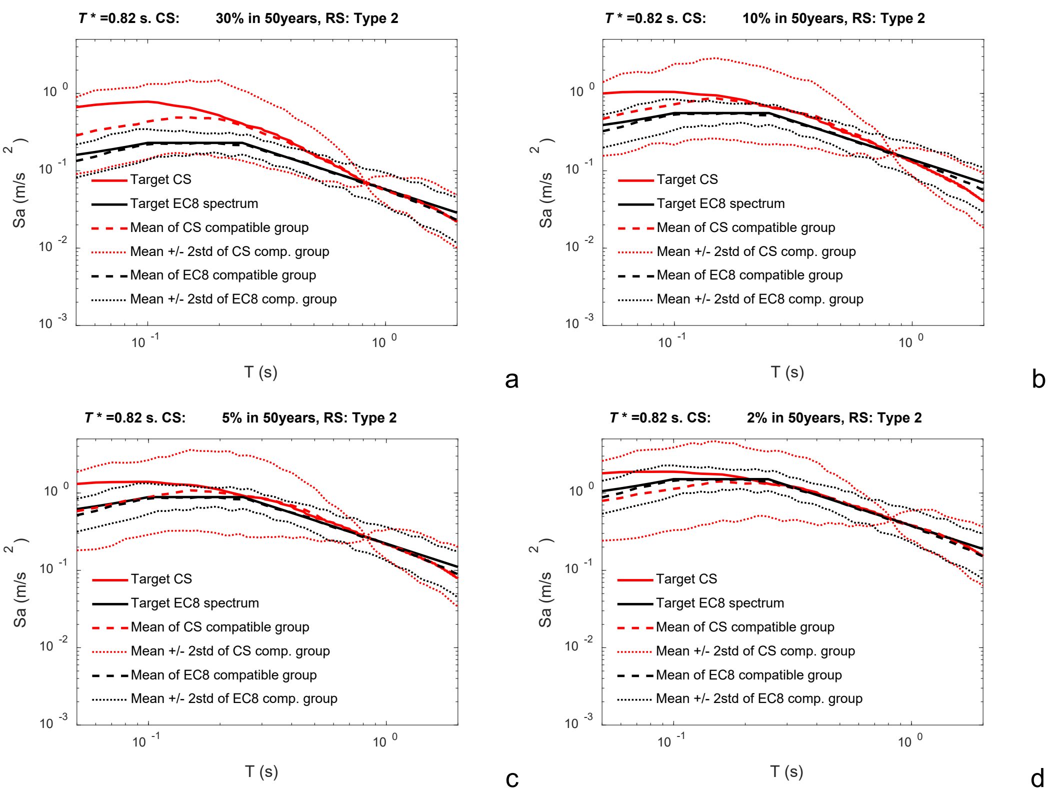

Figure 4. Comparison of response spectra (average and dispersion) of the group of GMs selected for the 5-storey building according to the CS (a. 30% in 50 years, b. 10% in 50 years, c. 5% in 50 years and d. 2% in 50 years) and the EC8 response spectrum. The target CS and EC8 spectrum are plotted for reference.

2.3. Probabilistic demand models

The two alternative PDMs obtained from the structural analyses are presented in this section, highlighting the implemented SFs. Both IDA and MSA analyses are performed using Sa(*T**) as the control IM. Structural collapse is associated to the occurrence of an infinitely large interstorey drift ISD (>10%) or numerical failure (non-convergence) of the model.

For the MSA, the four GM groups selected for each building are scaled up and down to span a total of 20 intensity levels. The GM group selected for the 50% probability of exceedance in 50 years was applied along 4 intensities (using group SFs in the range of 0.38-1.54), the 10% in 50 years group was applied along 3 intensities (using group SFs in the range of 0.82-1.23), the 5% in 50 years was applied along 4 intensities (using group SFs in the range of 0.89-1.39) and the 2% in 50 years was applied along 9 intensities (using group SFs in the range of 0.91-1.97), eventually covering events with return periods (RP) of ~50 to 10000 years. Detailed information on the SF and the RP can be found in Skoulidou et al. (2019). The overall SFs used for the GMs, which resulted from the combination of the group SFs and the individual SFs presented in Section 2.2, range from 0.11 to 7.84. IDA was performed by scaling the EC8 spectrum compatible group to capture structural response from elastic up to collapse. The SFs of the group ranged from 0.14 to 9.95. The overall SFs of the GMs (i.e., combination of the group SFs and the individual SFs presented in Section 2.2) range from 0.11 to 21.58, being almost three times higher than the SF used in MSA. The SFs employed for all GMs and all intensity levels for the two PDM are shown in Figure 5. Indicative analysis results (EDP-IM) obtained for the 3-storey building are presented in Figure 6 and in Figure 7 for the MSA (stripes of EDPs) and the IDA (IDA curves) PDM, respectively.

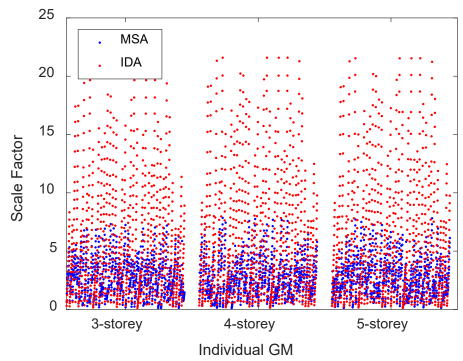

Figure 5 Overall SFs used for each GM and each intensity level for MSA and IDA.

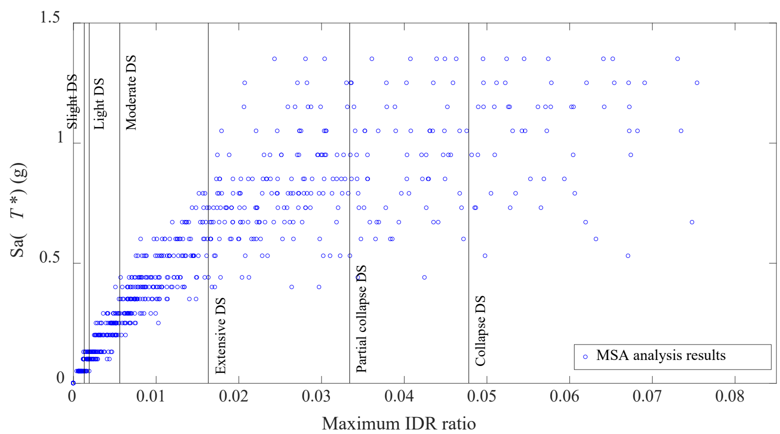

Figure 6. MSA analysis results (stripes) at the considered IM levels. Results for the 3-storey building. The vertical black lines represent the EDP thresholds for the considered damage states.

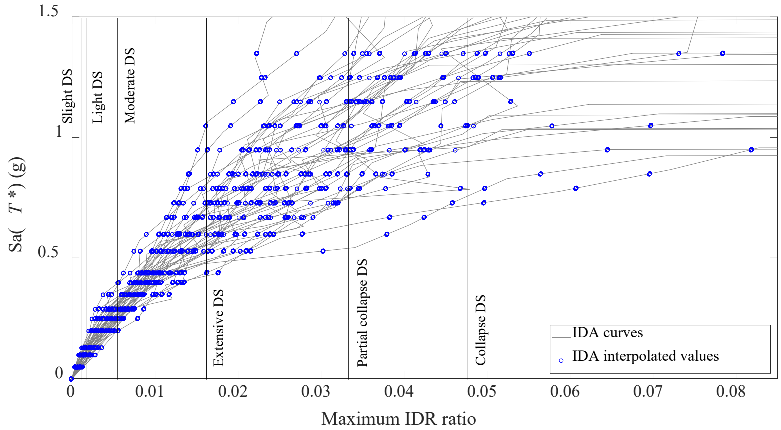

Figure 7. IDA curves and interpolated values at the considered IM levels. Results for the 3-storey building. The vertical black lines represent the EDP thresholds for the considered damage states.

3. Fragility curve development and comparison

3.1. Development of fragility curves

The EDP-based approach is used to fit fragility curves to the structural analysis results. According to this approach, the number of analyses that cause failure with respect to a predefined threshold at each IM level are initially identified and the binomial distribution is used to evaluate the likelihood of having the observed number of failures, k_i, out of the total number of analyses, n_i, at a given IM level i

$$\mathrm{P}(k_i failures\ in\ n_i analyses) = \binom{n_i}{k_i} {p_i}^{k_i}(1-p_i)^{n_i-k_i} \quad (1)$$

where p_i is the probability that an analysis at a given IM will lead to failure. When such data is available at multiple IM levels a likelihood function can be obtained as the product of the binomial probabilities at each IM level. The p_i, values are assumed to be defined by the cumulative distribution function of a lognormal distribution whose parameters are evaluated using the maximum likelihood estimation method. Furthermore, the maximum ISD ratio is used as the EDP and the thresholds of six Damage States (DS) are defined according to Rossetto and Elnashai (2003), shown in Table 3.

Table 3. Damage states definition and threshold values of maximum ISD ratios (Rossetto & Elnashai 2003).

Damage state	**Slight**	**Light**	**Moderate**	**Extensive**	**Partial Collapse**	**Collapse**
Max ISD ratio %	0.13	0.19	0.56	1.63	3.34	4.78

The adopted EDP-based fragility estimation requires that EDPs are obtained in distinct IM levels, i.e., in stripes. This requirement is satisfied by default in the MSA demand model (see Figure 6 for the 3-storey building), as GMs are selected for specific IM levels with predefined probabilities of exceedance, while in IDA some post processing of the PDM results needs to be performed. As such, the IDA curves are constructed for all GMs involved in the IDA demand model and are used to obtain EDP stripes at specific IM levels by interpolation. For consistency, interpolation was performed at the IM levels used for the MSA. It is noted that the IDA SFs presented in Figure 5 correspond to the SFs used to reach these IM levels. Figure 7 shows the IDA curves developed for the 3-storey building and the interpolated EDP values at the IM levels considered for the MSA of the same building. The vertical lines in Figure 7 represent the DS thresholds presented in Table 3.

Fragility curves are created for the three buildings according to the previously presented EDP-based approach for both MSA and IDA using a lognormal distribution for the six DSs. Figure 8, Figure 9 and Figure 10 show the fragility curves developed for the 3-storey, 4-storey, and 5-storey building, respectively. As a side note, it has been stated by Baker (2015), that for the estimation of the parameters of the lognormal distribution using the aforementioned approach, i.e., the maximum likelihood method, all GMs at the multiple IM levels should be independent. Nevertheless, according to the same author, the violation of this requirement has small effects on the estimated parameters and can be thus used even with IDA results, as in the present study (Baker, 2015).

3.2. Fragility curves comparison

It can be seen that for the three lower DSs, slight, light and moderate, there are insignificant differences between the fragility curves created using the IDA and the MSA PDM and this observation is valid for all three buildings analysed. Still, the MSA fragility curves exhibit an almost imperceptible shift towards conservatism. At the same time the fragility curves for these three DSs are quite vertical, i.e., they exhibit low dispersion. The reason for this low dispersion is attributed to the small number of stripes that contribute to the fragility curves of these DSs and their close values (the rest of the stripes lead to either 0 or 100% probability of exceedance). This effect is demonstrated in Figure 6 and Figure 7 which show the threshold EDP values for all DSs (vertical black lines) on top of the EDP stripes. The DS1 and DS2 EDP thresholds intersect only three stripes, while the DS3 EDP intersects four stripes, still with close Sa(*T**) values.

Despite the similarity of the fragility curves of these DSs (Slight, Light and Moderate) for the two alterative PDMs, the fractions of analysis causing failure for the individual IM values present differences. These differences can be seen in Figure 8, Figure 9 and Figure 10, which show the fractions of analyses that led to failure on top of the fitted curves. It can be observed that for DS1, DS2 and DS3 and for each individual IM that has not led to a 0 or 100% probability of failure, the MSA approach led to higher fractions compared to IDA. For instance, in Figure 10 and for the first IM which is equal to 0.05g, the fraction of analyses that led to failure according to MSA is 0.2, while for IDA it is less than 0.1. Similar observations can be made for the next two IMs, as well. It is also worth noting that these differences, i.e., the higher fractions of the MSA compared to IDA, can be associated with the GM spectral shapes presented in Section 2.2. The analysis of the four lowest stripes, that contribute to the development of the fragility curves of DS1 and DS2, was performed using the group compatible with the 30% in 50 years CS for the MSA. The comparison of this spectrum with that of the EC8 compatible group that was used to perform the IDA, shown in Figure 2a, Figure 3a and Figure 4a for the three buildings, reveals that, for spectral accelerations close to the period of vibration of the infilled structures (i.e., the period that the structures are expected to exhibit for these low IMs), the mean spectrum of the CS-compatible group is above the mean spectrum of the EC8-compatible group, while the dispersion of the former is much larger and mainly towards overestimation.

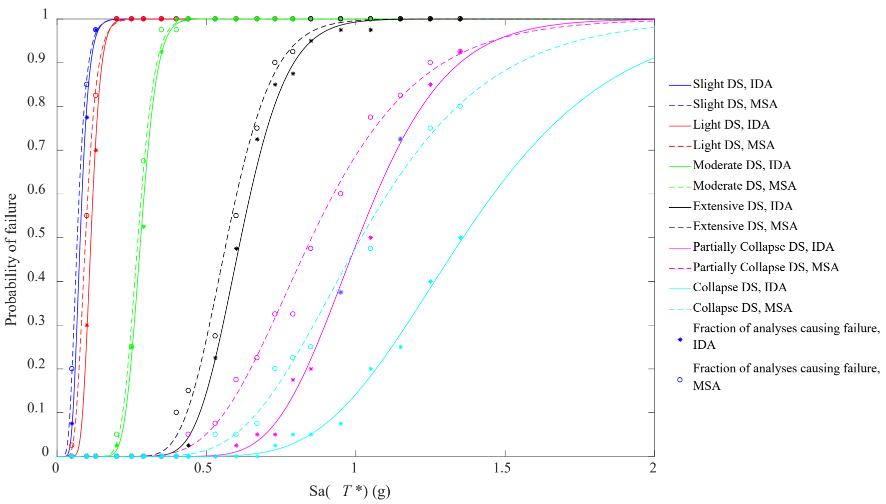

DS	MSA/IDA parameters θ	β
DS1	0.07/0.08	0.35/0.29
DS2	0.10/0.11	0.31/0.22
DS3	0.27/0.28	0.16/0.16
DS4	0.57/0.62	0.21/0.20
DS5	0.85/1.01	0.33/0.23
DS6	1.02/1.36	0.33/0.29

Figure 8. Fitted fragility curves and parameters of the lognormal model for the two alternative probabilistic demand models and the six DSs for the 3-storey building.

The discrepancies between the fragility curves created using the alternative PDMs are mainly observed for the three highest DS, i.e., extensive, partial collapse and collapse, with differences increasing with the severity of the DS and with different trends among the different buildings. The smallest differences are observed for the 5-storey building, presented in Figure 10. No remarkable differences can be seen for the fragility curves of the extensive DS, while the MSA PDM results in a slightly more conservative fragility curve for the partial collapse DS and in slightly higher dispersion for the collapse DS. Nevertheless, the observed differences can be characterised as minimal. These trends can be associated with the spectral shapes presented in Figure 4c and d, since the intensities that contribute to the fragility curves for these three DS are the ones associated with the 5% and 2% in 50 years CS for the MSA. For periods close to *T** and slightly larger than *T**, the two mean spectra are similar. Furthermore, the similar variation of the two groups around the mean spectra provides evidence for the similarity of the fragility curves. It is also noted that despite the much larger, almost three times, SFs used for the highest DS in IDA shown in Figure 5, no relevant overestimation is observed.

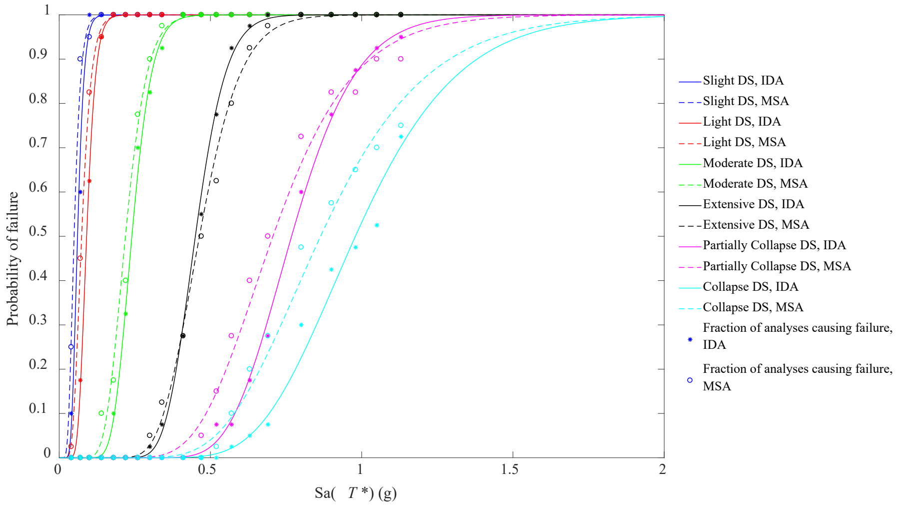

	MSA/IDA parameters	
DS	**θ**	**β**
DS1	0.05/0.06	0.35/0.28
DS2	0.07/0.09	0.34/0.26
DS3	0.22/0.24	0.25/0.22
DS4	0.46/0.45	0.23/0.18
DS5	0.71/0.76	0.29/0.22
DS6	0.86/0.98	0.31/0.27

Figure 9. Fitted fragility curves and parameters of the lognormal model for the two alternative probabilistic demand models and the six DSs for the 4-storey building.

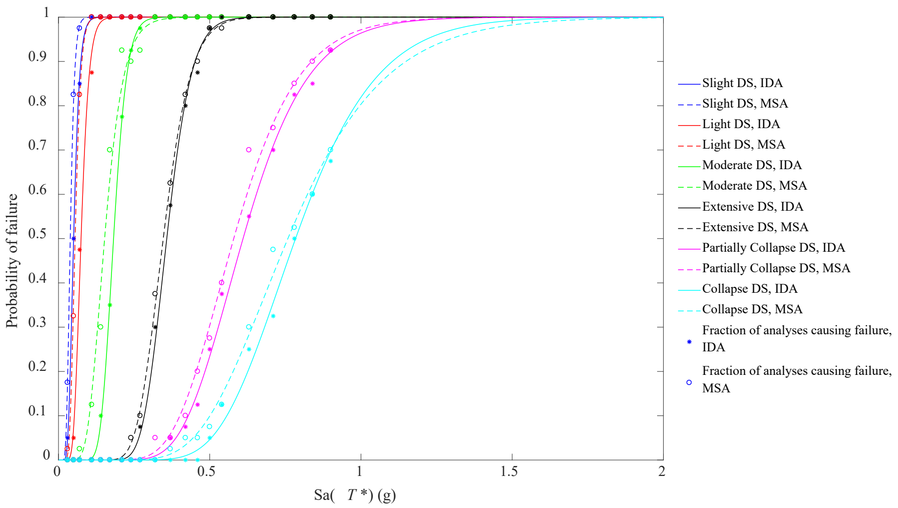

	MSA/IDA parameters	
DS	**θ**	**β**
DS1	0.04/0.05	0.28/0.30
DS2	0.05/0.07	0.27/0.28
DS3	0.15/0.18	0.31/0.19
DS4	0.35/0.36	0.21/0.18
DS5	0.58/0.61	0.29/0.27
DS6	0.76/0.78	0.32/0.27

Figure 10. Fitted fragility curves and parameters of the lognormal model for the two alternative probabilistic demand models and the six DSs for the 5-storey building.

The extensive DS fragility curves of the 3- and 4-storey buildings present small differences, the former in the median and the latter in the variability, while the partial collapse and the collapse DS fragility curves are the ones mostly affected by the alternative PDM. For both buildings, fragility curves derived using the MSA PDM are associated with lower IM levels, and are hence more conservative, while a slight difference in the slope is also observed for the partial collapse DS, with the MSA leading to higher dispersion (curves with lower slope). Based on the same rationale, the differences between the fragility curves of the 3-storey and the 4-storey buildings can be associated with the response spectra (mean and dispersion) of the 5% and 2% in 50 years probability of exceedance. In both cases, the average spectrum of the CS-compatible group presents slightly higher Sa values with respect to the average spectrum of the EC8-compatible group and for periods larger than, but close to, *T**. As it has already been explained, the buildings are expected to respond with periods closer to the bare frame, and thus larger than *T** for the higher intensities, as those associated with the DS of partial collapse and collapse. The variability of the group spectra is also higher for the CS compatible ones and always towards higher Sa values, hence further supporting the conservatism of the MSA PDM. The higher variability of the spectra of the CS-compatible groups can be reflected in the higher beta parameters of the lognormal model (i.e., the standard deviation of the logarithmic values) of the MSA fragility curves compared to their IDA counterparts. This effect is masked in the presented fragility curves which are plotted in the linear space. Last but not least, the much higher SFs used in IDA for the highest intensity levels do not seem to lead to overestimation of the corresponding fragility curves.

4. Final remarks

The study aimed at demonstrating differences between the fragility curves developed considering two alternative PDM, the MSA and the IDA. The referred differences were attributed only to the GM selection and scaling procedures since the same buildings were analysed in both cases and the same fitting technique was employed for the development of the fragility curves.

The results showed strong correlation between the mean spectra of the GM groups used for the two PDMs and the resulting fragility curves. The higher mean spectrum, i.e., higher Sa values, used for the MSA in comparison to the mean spectrum used for the IDA, appeared to translate into more conservative fragility curves for the former. Simultaneously, the higher variability of the CS compatible GMs was also reflected in the higher values of the beta parameter of the MSA-based fragility curves when compared to that obtained for the IDA-based fragility curves. Furthermore, the much higher SFs used on the GMs for IDA did not seem to have an observable effect on the fragility curves compared to the lower SFs used on the GMs for the MSA, unlike discussed in previous studies. The effect of the alternative PDM was found to vary among the different DSs and appeared to have minimal effects for the less severe DSs that were associated with highly vertical fragility curves. Although the spectral shapes might suggest otherwise, the small range of IMs that contributed to the fragility curves managed to reduce the impact of these differences. Still, the fractions of analyses used to create the fragility curves revealed the higher conservatism of the MSA compared to the IDA results, as suggested by the average spectra shape and their dispersion.

Overall, evidence was presented that both the mean spectral shape and the dispersion of the selected GM groups have an effect in the fragility curves and these were found to be the main sources of differences observed between the fragility curves developed for the alternative PDMs. The adoption of large SFs, on the other hand, did not seem to cause visible effects, as long as the spectral shape (average and dispersion) in the period range of interest was controlled. Although this was a preliminary attempt to identify and quantify the effects of using alternative PDMs, the results seem reasonable and in accordance with suggestions of relevant studies. Future research on this topic should investigate, in addition to the analysis of more buildings with different structural material and configurations (structural systems, with vertical and/or in-plan irregularities), fragility curves developed for the MSA and IDA using alternative fitting techniques (e.g., IM-based for IDA) and different PDMs (e.g., cloud analysis). Finally, the effect of using alternative PDMs could also be studied in terms of the resulting failure rates, i.e., the convolution of the fragility curves with the seismic hazard curve.

5. Acknowledgements/funding

The authors would like to thank Prof. Dimitrios Vamvatsikos for the fruitful discussions during the development of the presented manuscript. This work is financially supported by national funds through the FCT/MCTES (PIDDAC), under the project DRI/India/0645/2020 – Evaluation and Retrofitting of Existing Buildings for Safe and Sustainable Built Environment (https://doi.org/10.54499/DRI/India/0645/2020), and by Base Funding - UIDB/04708/2020 and Programmatic Funding - UIDP/04708/2020 of the CONSTRUCT - Instituto de I&D em Estruturas e Construções - funded by national funds through the FCT/MCTES (PIDDAC).

6. References

Baker, J. W. (2015). Efficient analytical fragility function fitting using dynamic structural analysis. Earthquake Spectra, 31(1), 579-599.

Baltzopoulos, G., Baraschino, R., Iervolino, I., & Vamvatsikos, D. (2018). Dynamic analysis of single-degree-of-freedom systems (DYANAS): A graphical user interface for OpenSees. Engineering Structures, 177, 395-408.

Chatzidaki, A., & Vamvatsikos, D. (2021). Mixed probabilistic seismic demand models for fragility assessment. Bulletin of Earthquake Engineering, 19(15), 6397-6421.

Dávalos, H., & Miranda, E. (2019). Evaluation of the scaling factor bias influence on the probability of collapse using Sa (T1) as the intensity measure. Earthquake Spectra, 35(2), 679-702.

Jalayer, F., & Cornell, C. A. (2009). Alternative non-linear demand estimation methods for probability-based seismic assessments. Earthquake Engineering & Structural Dynamics, 38(8), 951-972.

Jalayer, F., De Risi, R., & Manfredi, G. (2015). Bayesian Cloud Analysis: efficient structural fragility assessment using linear regression. Bulletin of Earthquake Engineering, 13, 1183-1203.

Jin, A., Qiu, Y., & Wang, J. (2023). Comparison of seismic fragility analysis methods for arch dams. Earthquake Engineering and Engineering Vibration, 22(1), 173-189.

Kohrangi, M., Vamvatsikos, D., & Bazzurro, P. (2017). Site dependence and record selection schemes for building fragility and regional loss assessment. Earthquake Engineering & Structural Dynamics, 46(10), 1625-1643.

Lin, T., & Baker, J. W. (2013). Introducing adaptive incremental dynamic analysis: a new tool for linking ground motion selection and structural response assessment.

Luco, N., & Bazzurro, P. (2007). Does amplitude scaling of ground motion records result in biased nonlinear structural drift responses?. Earthquake Engineering & Structural Dynamics, 36(13), 1813-1835.

Macedo, L., & Castro, J. M. (2017). SelEQ: An advanced ground motion record selection and scaling framework. Advances in Engineering Software, 114, 32-47.

Mackie, K. R., & Stojadinovic, B. (2005). Comparison of incremental dynamic, cloud, and stripe methods for computing probabilistic seismic demand models. In Structures Congress 2005: Metropolis and Beyond (pp. 1-11).

Pang, Y., & Wang, X. (2021). Cloud-IDA-MSA conversion of fragility curves for efficient and high-fidelity resilience assessment. Journal of Structural Engineering, 147(5), 04021049.

Rossetto, T., & Elnashai, A. (2003). Derivation of vulnerability functions for European-type RC structures based on observational data. *Engineering structures*, *25*(10), 1241-126.

Skoulidou, D., & Romão, X. (2019). Uncertainty quantification of fragility and risk estimates due to seismic input variability and capacity model uncertainty. Engineering Structures, 195, 425-437.

Skoulidou, D., Romão, X., & Franchin, P. (2019). How is collapse risk of RC buildings affected by the angle of seismic incidence?. Earthquake Engineering & Structural Dynamics; 48(14):1575-1594.

Vamvatsikos, D., & Cornell, C. A. (2002). Incremental dynamic analysis. Earthquake engineering & structural dynamics, 31(3), 491-514.

Zacharenaki, A., Fragiadakis, M., Assimaki, D., & Papadrakakis, M. (2014). Bias assessment in incremental dynamic analysis due to record scaling. Soil Dynamics and Earthquake Engineering, 67, 158-168.